Acta Biochim Biophys Sin 2010, 42: 548–557 | © The Author 2010. Published by ABBS Editorial Office in association with Oxford University Press on behalf of the Institute of Biochemistry and Cell Biology, Shanghai Institutes for Biological Sciences, Chinese Academy of Sciences. DOI: 10.1093/abbs/gmq059.
Advance Access Publication 5 July 2010

Original Article

Protective effects of a bacterially expressed NIF–KGF fusion protein against bleomycin-induced acute lung injury in mice

Xinping Li[1]*, Shengli Li[2], Miaotao Zhang[1], Xiukun Li[1], Xiaoming Zhang[1], Wenlong Zhang[1], and Chuanghong Li[1]

[1]Department of Animal Biotechnology, College of Veterinary Medicine, Northwest Sci-tech University of Agriculture and Forestry, Yangling 712100, China
[2]State Key Laboratory of Animal Nutrition, Beijing 100083, China
*Correspondence address. Tel: +86-29-87091201; Fax: +86-29-87091117; E-mail: lxp67cqu@163.com.

Current evidence suggests that the keratinocyte growth factor (KGF) and the polymorphonuclear leukocyte may play key roles in the development of lung fibrosis. Here we describe the construction, expression, purification, and identification of a novel NIF (neutrophil inhibitory factor)–KGF mutant fusion protein (NKM). The fusion gene was ligated via a flexible octapeptide hinge and expressed as an insoluble protein in *Escherichia coli* BL21 (DE3). The fusion protein retained the activities of KGF and NIF, as it inhibited both fibroblast proliferation and leukocyte adhesion. Next, the effects of NKM on bleomycin-induced lung fibrosis in mice were examined. The mice were divided into the following four groups: (i) saline group; (ii) bleomycin group (instilled with 5 mg/kg bleomycin intratracheally); (iii) bleomycin plus dexamethasone (Dex) group (Dex was given intraperitoneally (i.p.) at 1 mg/kg/day 2 days prior to bleomycin instillation and daily after bleomycin instillation until the end of the treatment); and (iv) bleomycin plus NKM group (NKM was given i.p. at 2 mg/kg/day using the same protocol as the Dex group). NKM significantly improved the survival rates of mice exposed to bleomycin. The marked morphological changes and increased hydroxyproline levels resulted from the instillation of bleomycin (on Day 17) in the lungs were significantly inhibited by NKM. These results revealed that NKM can attenuate bleomycin-induced lung fibrosis, suggesting that NKM could be used to prevent bleomycin-induced lung damage or other interstitial pulmonary fibrosis.

Keywords keratinocyte growth factor; neutrophil inhibitory factor; bleomycin; lung fibrosis; mice

Received: March 2, 2010 Accepted: May 13, 2005

Introduction

The keratinocyte growth factor (KGF) is a member of the fibroblast growth factor family and binds solely to its known high-affinity receptor (KGFR), which is exclusively localized on epithelial cells [1]. KGF produced by stromal cells is a critical growth factor in lung development and a protective agent after lung injury, indicating that it influences the interaction between epithelial and mesenchymal cells in a paracrine manner [2,3]. Overexpression of KGF in the lung results in papillary cystadenomas and enlargement of the bronchial airspaces [4]. Inhibiting the effects of KGF with a dominant-negative KGFR mutant results in the absence of branching morphogenesis within the developing lung [5]. The neutrophil inhibitory factor (NIF) is a hookworm-derived glycoprotein ligand of the CD11/CD18 integrin family that potently inhibits human neutrophil function *in vitro*, reduces leukocyte adhesion, decreases the number of neutrophils infiltrating tissues, and prevents *in vivo* neutrophil-dependent lung injury [6]. The recombinant NIF has been shown to markedly inhibit CD11/CD18-dependent human neutrophil function *in vitro* and *in vivo* [7,8]. Lung fibrosis is a pathological process characterized by injury and loss of lung epithelial cells and replacement of normal tissue by mesenchymal cells that produce an extracellular matrix [9]. The sequence of events leading to fibrosis of an organ involves subsequent injury processes, including inflammation, and disruption of the normal tissue architecture, followed by tissue repair and accumulation of mesenchymal cells in the area of derangement. The inflammatory cells play direct and indirect roles in tissue injury and repair. The early inflammatory phase is usually associated with the release of several cytokines and chemokines by activated resident cells and infiltrating cells [10]. Cytokines and growth factors secreted by inflammatory cells and interstitial cells (fibroblasts and myofibroblasts) play an important role in the fibrogenic phase of pulmonary fibrosis by inducing matrix synthesis [11]. Pulmonary fibrosis may be related to KGF and NIF. In this paper, we designed an NIF and KGF [neutrophil inhibitory factor–keratinocyte growth factor mutant fusion protein (NKM)] fusion protein linked by a flexible octapeptide

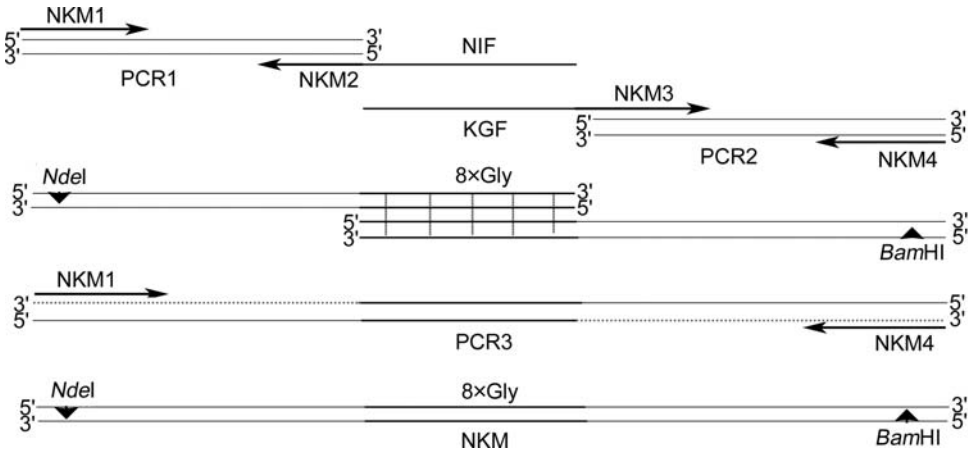

Figure 1 Construction and cloning of the NIF and KGF mutant fusion gene The NIF and KGF mutant gene (deletion of the 23 N-terminal amino acid residues in KGF) were cloned by PCR amplification using the forward and reverse primers NKM1 and NKM2, NKM3 and NKM4, respectively. The NKM fusion gene was constructed by ligating the above two PCR products using a third-round overlap PCR with the primers NKM1 and NKM4.

(G8) hinge to determine whether treatment with this protein can improve the outcome in the mice with bleomycin (BLM)-induced pulmonary fibrosis. We compared the fusion protein with dexamethasone (Dex), especially focusing on the acute phase of this model. We found that the fusion protein, but not Dex, showed a significant protective effect in this model, and possible mechanisms of action were discussed in the hope of discovering new pharmaceutical targets.

Materials and Methods

Expression vectors and reagents

A 774-bp segment encoding NIF (GenBank No. L27427.1) and a 423-bp segment encoding KGF (GenBank No. NM_002009.3, the full-length KGF coding sequence truncated by 69 bps at the N-terminus) were chemically synthesized by Chongqing Fagene Biomed Inc. (Chongqing, China), based on the codon bias for foreign gene expression in *Escherichia coli*. The expression vector pET-11c was purchased from Merck (Madison, USA). Gel extraction kits were from Shanghai Watson Biotech. (Shanghai, China).

Construction of expression plasmids for the NIF–KGF fusion

The strategy adopted in designing the recombinant plasmid vector expressing the NIF–KGF fusion protein is shown in **Fig. 1**. Three rounds of PCR were employed. A sequence encoding a flexible hinge octapeptide (GGGGGGGG) was fused to the 3′-end of the NIF gene and to the 5′-end of the KGF gene. A DNA fragment encoding NIF was amplified by PCR using NKM1 (5′-CGCATATGA ACGAACACAACTTGAGATGTCCACAAAACGGT-3′) as the forward primer and NKM2 (5′-TCCACCGCCTCCTCCA CCGCCTCCCAATTCTCTGAATCTGTA-3′) as the reverse primer, resulting in a 24-bp oligonucleotide sequence encoding a flexible glycine octapeptide hinge (GGGGGGGG) at the 3′-end. A DNA fragment encoding the KGF mutant was synthesized by PCR using NKM3 (5′-GGAGGCGGTG GAGGAGGCGGTGGATCTTACGACTACATGGAA-3′) as the forward primer and NKM4 (5′-CGGATCCTCAGG TGATAGCCATCGGCAGGAAGTGAGCGGT-3′) as the reverse primer, resulting in a 24-bp oligonucleotide sequence encoding a flexible glycine octapeptide hinge at the 5′-end of the KGF mutant. The two PCR products were purified and joined together using an overlap PCR with NKM1 as the forward primer and NKM4 as the reverse primer. The PCR product was purified, digested with *Nde*I–*Bam*HI, and subcloned into the pET-11c vector treated with the corresponding enzymes. The identity of the insert was confirmed via sequencing, and the expression construct was designated pET-NKM.

Expression, refolding, and purification of the recombinant protein and western blot analysis

Competent *E. coli* strain BL21 (DE3) plysS Star bacteria (Invitrogen, Carlsbad, USA) was transformed with the plasmid pET-NKM, and the resulting transformants were selected on LB (Luria–Bertani) agar plates containing 100 μg/ml ampicillin. For large-scale expression and purification, 300 ml of starter culture with a recombinant NKM colony was added to 2 l of LB medium (pH 7.0) containing 100 μg/ml ampicillin at 37°C in a 3 l fermenter. When the OD_{600} reached 5.0, recombinant NKM expression was induced by adding IPTG to a final concentration of 0.5 mM and the fermentation was continued for 3 h. The cells were harvested and suspended in 1 l lysis buffer, and then sonicated using an ultrasonic disintegrator for 40 cycles (4 s per cycle). The inclusion bodies (IBs) were sedimented by

centrifugation, followed by three more washes in water containing 2 M urea buffered with 50 mM Tris base (pH 10.5). The resulting IB pellet was solubilized in 8 M urea buffer until the solution became clear, and then applied to a Fast-Flow DEAE-Sepharose column (Amersham, Uppsala, Sweden) in an AKTA primer purifier (Amersham). The sample was eluted using a discontinuous gradient of 0.1–0.3 M NaCl in the same buffer. Positive fractions were identified by western blotting. The purified fusion protein was dialyzed overnight and diluted with 20 volumes of 50 mM Tris, pH 9.5 (0.5% sodium dodecyl sulfate (SDS) was added). The target protein was precipitated by adjusting the pH to its isoelectric point (6.1), concomitantly removing the SDS using isopropyl alcohol, and then centrifuging at 12,900 *g* for 15 min at 4°C. The protein concentration was determined by the Lowry method. SDS–Polyacrylamide gel electrophoresis (PAGE) was carried out according to Laemmli [12] in a 15% polyacrylamide gel under reducing conditions for determining the relative molecular mass, and under non-reducing conditions to test the purity and monomeric nature of the samples. The N-terminal amino acid sequence was determined by Edman degradation at the Research Center for Proteome Analysis, Institute of Biochemistry and Cell Biology, SIBS, CAS. Western blotting was performed using rabbit polyclonal anti-NIF (1:500 dilution) and anti-KGF (1:400 dilution) serum (Chongqing Fagene Biomed Inc.), and anti-rabbit IgG conjugated with horseradish peroxidase (1:500 dilution) (Zhongshan Goldenbridge Biotechnology, Beijing, China). The peroxidase activity was detected using 3,3-diaminobenzidine. The reaction was stopped by washing with double-distilled water as described by Ma *et al*. [13]. The resulting picture was scanned with a GIS-700D imaging system.

In vitro bioactivity assay of the recombinant protein

Blood was withdrawn from the hearts of male New Zealand white rabbits (2.5–3.0 kg) and the leukocytes were purified by gradients of Percoll as described [14]. The resultant white cell pellet was suspended in RPMI 1640 medium containing 1% human serum albumin (HSA). The adhesion inhibition activity of the NKM fusion protein was assayed by the quadruple serial dilution method in RPMI 1640 containing 2.4 mM $CaCl_2$, 2.0 mM $MgCl_2$, 1% HSA, and 1 μM phorbol myristate acetate (PMA; Sigma, St Louise, USA) over the range of 24.4 ng/ml–100.0 μg/ml. The assay was performed as described by Bullido *et al*. [15] with some modifications. Briefly, 96-well microtiter plates (Costar, New York, USA) were plated with 50 μl of cell suspension and 50 μl of the serially diluted fusion protein in triplicate. After 1 h of incubation, the non-adherent cells were removed by washing and the adherent cells were stained with 0.5% crystal violet, washed with PBS, and lysed with 1% TritonX-100. The degree of adhesion inhibition was determined by comparing OD_{630} values with those of control cells (cells not exposed to the NKM fusion protein). The percentage of adherent cells was calculated.

The effect of the NKM fusion protein on the viability of NIH/3T3 cells was assessed using the MTT assay. NIH/3T3 cells ($6 \times 10^4 - 8 \times 10^4$ cells/ml) were plated in 96-well plates and grown in DMEM (Gibco, Grand Island, USA) supplemented with 10% (*v*/*v*) heat-inactivated fetal bovine serum (Hyclone, Logan, USA) in a 5% CO_2 humidified incubator at 37°C for 24 h. Then the medium was removed and replaced with 0.1 ml of fresh medium containing different concentrations of the NKM fusion protein (3.9 − 500 μg/ml). All the experiments were carried out in triplicate. After incubation for another 24 h, 20 μl of MTT solution (Fluka, Buchs, Switzerland) was added. The plates were further incubated for 6.5 h at 37°C. The resulting formazan product was dissolved in 120 μl of acidified isopropanol, and the absorbance was measured at 630 nm.

In vivo effect of the recombinant protein

All animal-based experimental procedures were performed in accordance with the ethical guidelines stated in the Guide for the Use and Care of Laboratory Animals in China. Female Kunming strain mice (weighing 23–27 g) were purchased from the Laboratorial Animals Center in Xi'an Jiao Tong University. After acclimation, the mice were then randomly divided into the following four groups: (i) saline group ($n = 8$); (ii) BLM alone group ($n = 8$)—animals were intratracheally instilled with 5 mg/kg BLM solution (Nippon Kayaku, Tokyo, Japan) (2.5 mg/ml in 0.9% sterile saline); (iii) BLM + Dex group ($n = 12$)—animals were intraperitoneally (i.p.) given Dex at 1 mg/kg/day 2 days prior to BLM instillation and daily after BLM instillation until the end of the treatment; and (iv) BLM + NKM group ($n = 12$)—animals were i.p. given NKM dissolved in 0.9% sterile saline at 2 mg/kg/day using the same protocol as the Dex group. The animals were shaken to facilitate the distribution of the BLM and saline [16]. On day 17 after administration, animals were euthanized, and whole blood was taken and collected into anticoagulant (EDTA)-containing tubes. Total and differential peripheral leukocyte counts were measured. Pulmonary fibrosis was assessed based on lung hydroxyproline content and histological changes. The lung tissues were fixed with a buffered 15% formalin solution for 1 week, embedded in paraffin, and then sectioned at 3 μm. The sections were stained with hematoxylin and eosin (H&E) and Masson trichrome, and α-smooth muscle actin (α-SMA) expression was detected by immunohistochemical assay.

Statistical analysis

The data are expressed as the mean ± SD. The data from the cell bioactivity assays were analyzed by linear

regression of the different concentrations of the NKM against inhibition activity (specified as $\ln OD_{630}$ value), and the differences between the differential blood counts and lung hydroxyproline levels among the groups were evaluated by ANOVA followed by the *F*-test and Fisher's LSD test. Statistical analysis of mortality among the groups was carried out by the χ^2 test. A probability value of <0.05 was considered statistically significant for all data.

Results

Cloning and sequencing the NKM fusion gene

Using the three-primers PCR method, we anchored the gene fragment encoding the KGF mutant at the 3′-end of the NIF gene to form a fusion gene. This was then inserted into the T vector. To support the natural conformations of NIF and the KGF mutant, a flexible octapeptide (G_8) hinge was introduced between the two peptides (**Fig. 1**). The PCR product was purified and digested with *Bam*HI and *Nde*I and then subcloned into the expression vector pET-11c, which had been digested using the same restriction enzymes. The results of double enzyme digestion and PCR amplification showed that the fusion gene encoding NKM was inserted into the pET-11c vector correctly (**Fig. 2**). The identity of the fusion gene was confirmed by sequencing, and the full-length nucleotide and deduced amino acid sequences are shown in **Fig. 3**. Taken together, these results demonstrate that the NKM fusion gene was constructed successfully.

Expression, purification, and western blot assay of the recombinant protein

Recombinant protein expression was achieved in *E. coli* using the pET system. To purify the protein, a Fast-Flow DEAE-Sepharose column was applied. Under reducing and non-reducing conditions, the purified recombinant protein yielded a single band of 46 kDa (**Fig. 4**) on an SDS–PAGE gel after Coomassie blue staining. The active monomer molecules were enriched. The N-terminal 15 amino acids were Met-Asn-Glu-His-Asn-Leu-Arg-Cys-Pro-Gln-Asn-Gly-Thr-Glu-Met, in agreement with the natural amino acid sequence of NIF. Furthermore, western blot analysis showed that primary antibodies recognizing NIF and the KGF mutant also recognized the purified fusion protein, forming bands of 30.6, 16, and 46.6 kDa, respectively (**Fig. 5**). These results indicated the presence of the recombinant NKM protein.

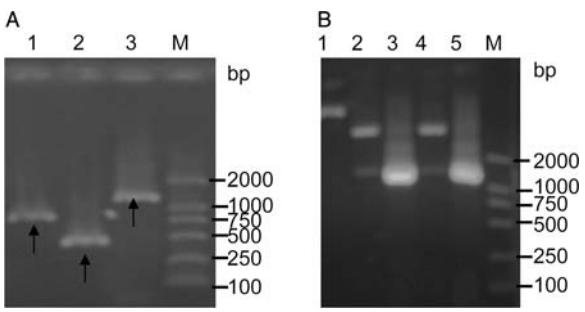

Figure 2 Identification of the expression vector pET-NKM Lane M represents the DL 2000 DNA Marker A. (A) Lane 1, the NIF gene; lane 2, the KGF mutant gene; and lane 3, the NKM gene. The arrows indicate the presence of the target gene fragments. (B) Lane 1, the recombinant plasmid undigested with *Nde*I and *Bam*HI; lanes 2 and 4, the recombinant plasmid digested with *Nde*I and *Bam*HI; and lanes 3 and 5, the NKM PCR product using the recombinant plasmid pET-NKM as the template.

NKM inhibits polymorphonuclear leukocyte adhesion

The ability of the NKM to inhibit polymorphonuclear leukocyte (PMN) binding was determined using an *in vitro* plate assay. As presented in **Fig. 6**, the inhibition of adhesion and the concentration of the NKM correlated well, with $r = -0.81$ by single linear regression analysis. This close correlation indicated that NKM prevented the binding of PMA-activated PMNs to the plate in a dose-dependent manner. NKM at 100 μg/ml inhibited PMN adhesion in response to PMA by ~56%. The inhibition of PMN adhesion was also observed at an NKM concentration of 24.4 ng/ml, reaching 23%. This indicated that the NKM reproduced the effect of NIF that can inhibit PMN adhesion.

NKM inhibits NIH3T3 cells proliferation

To determine whether NKM inhibits cellular proliferation, an MTT assay was performed. The optical density values representing NKM inhibitory activity were measured, and the subsequent analysis used natural logarithms to assess the correlation with NKM concentration by linear regression. Linear regression analysis of the data revealed a highly negative correlation between inhibitory activity and increasing concentration ($r = -0.94$). NKM inhibited the proliferation in a dose-dependent manner (**Fig. 7**), further suggesting that NKM possesses the function of the KGF.

Mortality

Out of eight mice in the BLM group, seven died. This 87.5% cumulative mortality was reduced to 25% in the BLM + NKM group, as only three mice died out of 12 in this group, indicating NKM could reverse the high mortality caused by BLM. Nine of the 12 mice (75%) in the Dex + BLM group died over the course of the study, suggesting Dex did not improve the survival rate. In the saline group, two mice out of eight died.

Total and differential cell counts in whole blood

The total and differential cell counts in whole blood from various groups are shown in **Table 1**. There was no difference in total cell count between mice in the BLM + NKM and Dex + BLM groups, and this count was lower than that of the saline control group. However, the difference was not statistically significant. The differential cell counts

```
   1 ATGAACGAACACAACTTGAGATGTCCACAAAACGGTACTGAAATGCCAGGTTTCAACGAC  60
   1  M  N  E  H  N  L  R  C  P  Q  N  G  T  E  M  P  G  F  N  D  20
  61 TCCATCAGATTGCAATTCTTGGCTATGCACAACGGTTACAGATCCAAGTTGGCTTTGGGT 120
  21  S  I  R  L  Q  F  L  A  M  H  N  G  Y  R  S  K  L  A  L  G  40
 121 CACATCTCCATCACTGAAGAATCCGAATCCGACGACGACGACGACTTCGGTTTCTTGCCA 180
  41  H  I  S  I  T  E  E  S  E  S  D  D  D  D  D  F  G  F  L  P  60
 181 GACTTCGCTCCAAGAGCTTCCAAGATGAGATACTTGGAATACGACTGTGAAGCTGAAAAG 240
  61  D  F  A  P  R  A  S  K  M  R  Y  L  E  Y  D  C  E  A  E  K  80
 241 TCCGCTTACATGTCCGCTAGAAACTGTTCCGACTCCTCCTCCCCACCAGAAGGTTACGAC 300
  81  S  A  Y  M  S  A  R  N  C  S  D  S  S  S  P  P  E  G  Y  D 100
 301 GAAAACAAGTACATCTTCGAAAACTCCAACAACATCTCCGAAGCTGCTTTGAAGGCTATG 360
 101  E  N  K  Y  I  F  E  N  S  N  N  I  S  E  A  A  L  K  A  M 120
 361 ATCTCCTGGGCTAAGGAAGCTTTCAACTTGAACAAGACTAAGGAAGGTGAAGGTGTTTTG 420
 121  I  S  W  A  K  E  A  F  N  L  N  K  T  K  E  G  E  G  V  L 140
 421 TACAGATCCAACCACGACATCTCCAACTTCGCTAACTTGGCTTGGGACGCTAGAGAAAAG 480
 141  Y  R  S  N  H  D  I  S  N  F  A  N  L  A  W  D  A  R  E  K 160
 481 TTCGGTTGTGCTGTTGTTAACTGTCCATTGGGTGAAATCGACGACGAAACTAACCACGAC 540
 161  F  G  C  A  V  V  N  C  P  L  G  E  I  D  D  E  T  N  H  D 180
 541 GGTGAAACTTACGCTACTACTATCCACGTTGTTTGTCACTACCCAAAGATCAACAAGACT 600
 181  G  E  T  Y  A  T  T  I  H  V  V  C  H  Y  P  K  I  N  K  T 200
 601 GAAGGTCAACCAATCTACAAGGTTGGTACTCCATGTGACGACTGTTCCGAATACACTAAG 660
 201  E  G  Q  P  I  Y  K  V  G  T  P  C  D  D  C  S  E  Y  T  K 220
 661 AAGGCTGACAACACTACTTCCGCTGACCCAGTTTGTATCCCAGACGACGGTGTTTGTTTC 720
 221  K  A  D  N  T  T  S  A  D  P  V  C  I  P  D  D  G  V  C  F 240
 721 ATCGGTTCCAAGGCTGACTACGACTCCAAGGAGTTCTACAGATTCAGAGAATTGGGAGGC 780
 241  I  G  S  K  A  D  Y  D  S  K  E  F  Y  R  F  R  E  L  G  G 260
 781 GGTGGAGGAGGCGGTGGATCTTACGACTACATGGAAGGTGGTGACATCCGTGTTCGTCGT 840
 261  G  G  G  G  G  G  S  Y  D  Y  M  E  G  G  D  I  R  V  R  R 280
 841 CTGTTCTGCCGTACCCAGTGGTACCTGCGTATCGACAAACGTGGTAAAGTTAAAGGTACC 900
 281  L  F  C  R  T  Q  W  Y  L  R  I  D  K  R  G  K  V  K  G  T 300
 901 CAGGAAATGAAAAACAACTACAACATCATGGAAATCCGTACCGTTGCTGTTGGTATCGTT 960
 301  Q  E  M  K  N  N  Y  N  I  M  E  I  R  T  V  A  V  G  I  V 320
 961 GCTATCAAAGGTGTTGAATCTGAGTTCTACCTGGCTATGAACAAAGAAGGTAAACTGTAC 1020
 321  A  I  K  G  V  E  S  E  F  Y  L  A  M  N  K  E  G  K  L  Y 340
1021 GCTAAAAAAGAATGCAACGAAGACTGCAACTTCAAAGAACTGATCCTGGAAAACCACTAC 1080
 341  A  K  K  E  C  N  E  D  C  N  F  K  E  L  I  L  E  N  H  Y 360
1081 AACACCTACGCTTCTGCTAAATGGACCCACAACGGTGGTGAAATGTTCGTTGCTCTGAAC 1140
 361  N  T  Y  A  S  A  K  W  T  H  N  G  G  E  M  F  V  A  L  N 380
1141 CAGAAAGGTATCCCGGTTCGTGGTAAAAAAACCAAAAAAGAACAGAAAACCGCTCACTTC 1200
 381  Q  K  G  I  P  V  R  G  K  K  T  K  K  E  Q  K  T  A  H  F 400
1201 CTGCCGATGGCTATCACCTGA                                        1221
 401  L  P  M  A  I  T  *                                          406
```

Figure 3 Nucleotide and deduced amino acid sequences of NKM The linker octapeptide between the NIF gene and the KGF mutant is underlined. The '*' indicates a stop codon.

showed that treatment with NKM or Dex significantly reduced neutrophil numbers compared with saline treatment. Furthermore, mice treated with NKM or Dex had significantly lower numbers of lymphocytes and mid-cells comparing with those treated with saline alone. There was no difference between mice treated with NKM and Dex.

Assessment of pulmonary fibrosis

Lung collagen levels, as assessed by hydroxyproline content, were presented in **Fig. 8**. Treatment with BLM alone produced a significant increase in hydroxyproline levels when compared with the controls that received normal saline. NKM and Dex treatment prevented the increase in hydroxyproline content caused by BLM treatment after 17 days, but there was no difference between Dex and NKM treatment.

Histopathology examination

Histological examination of the lungs from saline-treated mice [**Fig. 9(A)**] revealed normal bronchiolar epithelium, thin interalveolar septa, a lack of inflammatory cells, and fibrosis. This also showed normal alveolar spaces and normal thickening of the alveolar septa. Mice treated with BLM alone showed collapsed and narrow alveolar spaces [**Fig. 9(B)**]. The pulmonary interstitium was markedly infiltrated with inflammatory cells and fibroblasts in the mice treated with BLM alone, leading to thickening of the interalveolar septa. The lungs from mice in the BLM + NKM group [**Fig. 9(C)**] showed thick interalveolar septa similar to those of the saline-instilled mice, no infiltration of inflammatory cells, and a clear diminution of the fibrotic lesions. The lungs from mice in the BLM + Dex group had fewer fibrotic lesions than the mice in the BLM group,

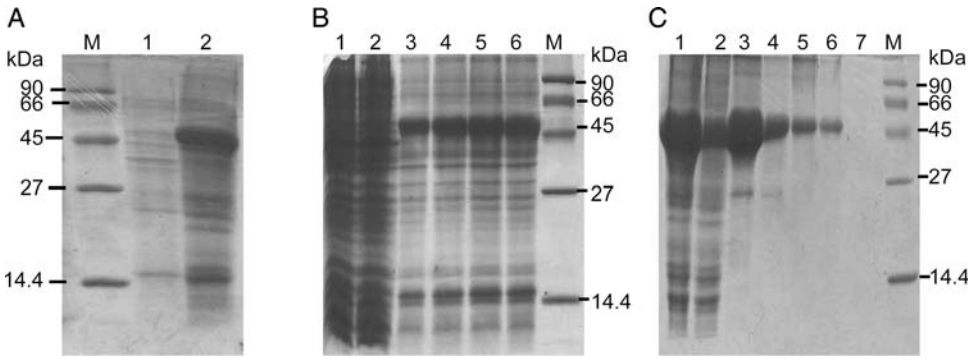

Figure 4 SDS–PAGE analysis of NKM expression in *E. coli* Lane M, intermediate molecular weight protein standard. (A) Lane 1, total cellular extract before induction; lane 2, total cellular extract from IPTG-induced *E. coli* BL21 (DE3) containing pET-NKM. (B) Lane 1, total cellular extract from *E. coli* BL21 (DE3) not containing pET-NKM; lane 2, total cellular extract containing pET-NKM before induction; and lanes 3–6, total cellular extracts of IPTG-induced *E. coli* BL21 (DE3) containing pET-NKM for 1, 2, 3, and 4 h, respectively. (C) Lane 1, the insoluble fraction before purification; lane 2, the flow-through peak from the Fast-Flow DEAE-Sepharose column; and lanes 3–7, the active peaks eluted using 0.1, 0.15, 0.2, and 0.3 M NaCl, respectively.

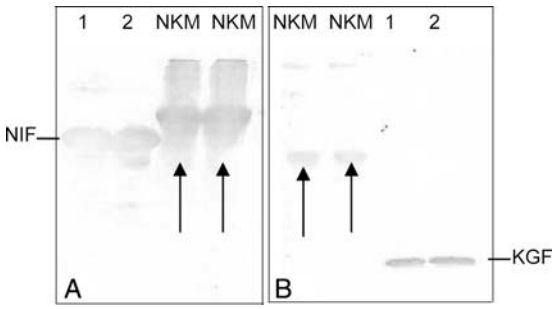

Figure 5 Western blot analysis of NKM expressed in *E. coli* Purified NIF and KGF were transferred onto nitrocellulose membrane from an SDS gel and blotted with rabbit anti-NIF and anti-KGF sera. Anti-rabbit IgG conjugated with HRP was used as the secondary antibody. (A) Lanes 1 and 2, purified recombinant NIF protein binding to rabbit anti-NIF serum. (B) Lanes 1 and 2, purified recombinant KGF protein binding to rabbit anti-KGF serum. The arrows indicate binding of the NKM fusion protein to the rabbit anti-NIF and KGF sera.

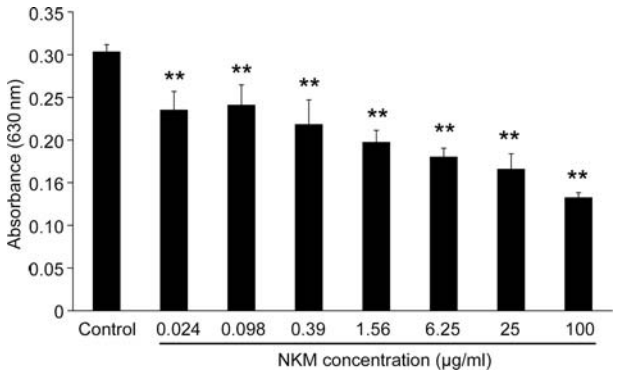

Figure 6 NKM prevents binding of PMNs to plate glass PMNs were layed onto a plate surface and immediately activated by treatment with PMA (1 μM for 1 h) in the absence (control column) or presence of the indicated concentrations of recombinant NKM Ln OD_{630} showed a linear correlation with NKM concentration (with a correlation coefficient of $r = -0.81$). NKM inhibited the binding of PMNs to the plate in a dose-dependent manner. Data are expressed as mean ± SD of three separate experiments. $^{**}P < 0.01$ compared with the control.

and moderate thickening of the interalveolar septa was observed [**Fig. 9(D)**]. In addition, there was an excessive amount of collagen deposited around the alveoli in the lungs of the BLM-treated mice, as revealed by Masson trichrome staining [**Fig. 9(F)**]. Mice in BLM + NKM showed marked suppression of the BLM-induced collagen accumulation, as evidenced by reduced thickening of the interalveolar septa on Day 17 compared with the lungs of BLM-treated mice [**Fig. 9(G)**]. However, slight interstitial wall thickening was observed in the BLM + Dex group [**Fig. 9(H)**]. Next, the correlation between α-SMA expression and fibrosis was assessed. In the BLM-treated mice, α-SMA expression in the lungs was observed [**Fig. 9(J)**]. This was significantly reduced in the BLM + NKM mice to the level found in the control saline-treated mice [**Fig. 9(K)**]. On the 17th day after BLM treatment, modest expression of α-SMA was found in the BLM + Dex group [**Fig. 9(L)**]. These results suggest that markedly suppressed expression of α-SMA is associated with the improvement of BLM-induced lung fibrosis after NKM treatment.

Discussion

The KGF is almost exclusively synthesized by mesenchymal cells, particularly fibroblasts, and it can protect epithelial cells from various insults through the KGFR expressed on these cells [17]. Recombinant human KGF (rHuKGF, ΔN23-KGF) expressed in *E. coli* (palifermin) has been demonstrated to provide highly significant amelioration of the radiation-induced mucosal response when applied at the onset of clinical mucositis [18]. Deletion of the 23 N-terminal amino acid residues in the KGF increases the stability of the protein but does not affect its

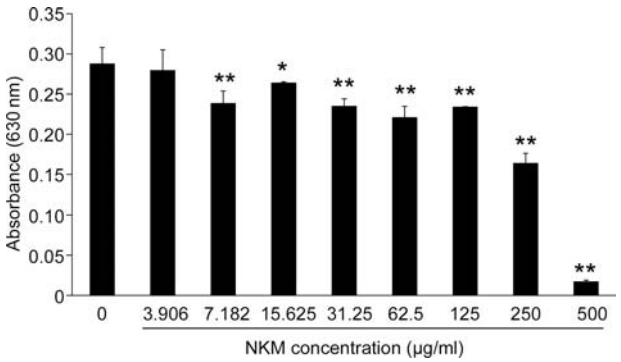

Figure 7 NKM inhibits NIH3T3 cells proliferation After treatment of NIH3T3 cells for 24 h with various doses of NKM (3.9 − 500 μg/ml), cell proliferation was assessed by MTT assay. Data are expressed as mean ± SD of three independent experiments. The effect of the NKM on cell viability was described by linear regression (with a correlation coefficient of $r = -0.94$). $^{*}P < 0.05$, $^{**}P < 0.01$ compared with the control.

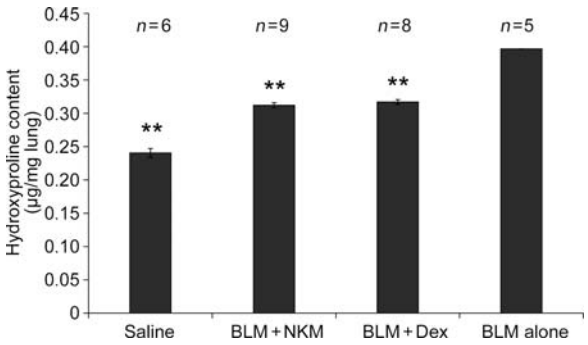

Figure 8 NKM-treated mice had lower lung hydroxyproline levels BLM treatment significantly increased the hydroxyproline content in the lung tissue of mice compared with lungs of control mice receiving saline. NKM and Dex both significantly decreased the hydroxyproline levels in the lung tissue of mice induced by BLM. The number of animals in each group is noted. Values are expressed as mean ± SD. $^{**}P < 0.01$ compared with the BLM alone group.

activity in a Balb/MK epidermal keratinocyte cell line [19]. When administered intratracheally, KGF acts as a potent mitogen of alveolar epithelial type II cells, and the production of surfactant protein A associated with the tubular myelin fraction of the intra-alveolar surfactant increased by 47% in comparison with buffer-treated control lungs. In contrast, intra-alveolar surfactant subtypes were not affected [20]. However, we found in our previous study that the analog can inhibit the proliferation of fibroblasts markedly in a dose-dependent manner (data not shown), consistent with results of Tang and Gilchrest [21]. In the present study, a fusion protein connecting NIF and N23-KGF via a flexible octapeptide (G8) hinge behaved identically (**Fig. 7**). This may be one of the mechanisms by which KGF prevents the generation of lung fibrosis. However, the rapid accumulation of neutrophils in the lung is one of the first recognizable events in response to inflammatory stimuli, and it plays a critical role in the pathogenesis of many pulmonary diseases such as acute lung injury, acute respiratory distress syndrome, and lung fibrosis. The process by which neutrophils cross the pulmonary vasculature, migrate through the lung interstitium, and ultimately accumulate in the airways requires complex interactions between circulating leukocytes and the cells of the lung [22]. NIF, a 41-kDa CD11/CD18 β2 integrin-binding protein isolated from the canine hookworm (*Ancylostoma caninum*), specifically blocks PMN adhesion to endothelial cells, infiltration into the lungs, and migration responses in a concentration-dependent manner [23]. Recombinant NIF can inhibit PMN adhesion in a concentration-dependent fashion (data not shown). Therefore, expression of the NIF and KGF mutant fusion protein is a practical strategy for preventing lung fibrosis. Recombinant NIF–KGF fusion protein has not previously been reported in either *E. coli*, insect, potato, tomato, or tobacco [24]. Here, we report the cloning and expression of the NIF–KGF mutant fusion gene in *E. coli* BL21 (DE3). The recombinant NKM fusion protein not only has the same proliferation-inhibitory activity as the KGF mutant (**Fig. 7**), but it also plays the same role as NIF (**Fig. 6**). However, NKM cannot fully abrogate PMN adhesion *in vitro*.

Consequently, we tested purified NKM in a BLM-induced animal model of lung fibrosis. BLM causes inflammatory and fibrotic reactions in the lungs of mice within a short period after intratracheal instillation, leading

Table 1 Effect of NKM on BLM-induced changes in total and differential cell counts in blood from mice

Treatment group	*n*	Total cells ($\times 10^9$/L)	Neutrophils ($\times 10^9$/L)	Mid cell ($\times 10^9$/L)	Lymphocytes ($\times 10^9$/L)
Saline	6	7.00 ± 1.20	1.38 ± 0.36	0.58 ± 0.11	5.05 ± 0.92
BLM	1	10.2	1.3	0.9	8
BLM + NKM	8	5.79 ± 1.01	0.54 ± 0.17	0.39 ± 0.11	4.96 ± 0.76
BLM + Dex	3	5.54 ± 1.31	0.74 ± 0.13	0.31 ± 0.16	4.67 ± 1.18

Data presented as mean ± SD. BLM, bleomycin; NKM, neutrophil inhibitory factor–keratinocyte growth factor mutant fusion protein; Dex, dexamethasone.

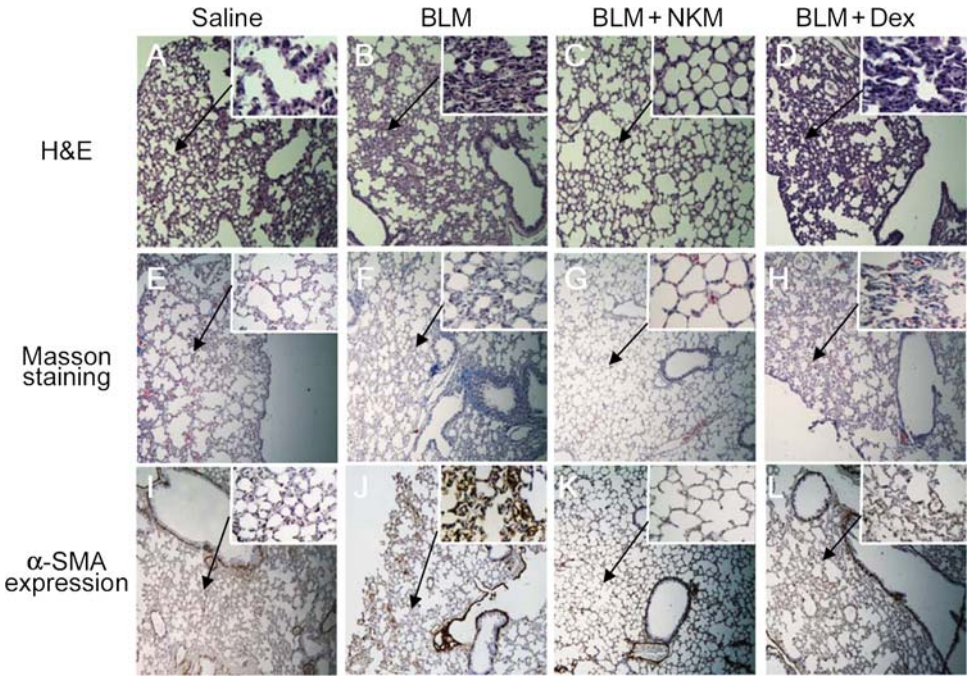

Figure 9 NKM significantly prevented the BLM-induced histological changes in mouse lungs (A) The normal histological appearance of the lung stained with H&E (saline). (B) Extensive fibrosis (BLM). (C) Marked prevention of the BLM-induced histological changes in mouse lungs by NKM and (D) Dex. The lungs were stained with Masson trichrome and detected for the expression of α-SMA in mice with anti-α-SMA antibody. BLM-treated mice showed excessive collagen deposition (F) and the expression of α-SMA in their interstitial lung tissue (J). NKM plus BLM treatment led to a marked reduction in the interstitial deposition of collagen (G) and suppression of α-SMA (K). Dex plus BLM treatment resulted in a moderate reduction of the interstitial deposition of collagen (H) and suppression of α-SMA (L). The arrows indicate the locations of the inset photographs. Magnification, 400×.

to histological features similar to those of human lung diseases [25]. Chaudhary *et al*. [26] reported the pathological features of BLM-induced acute lung injury and fibrosis, including alveolitis and interstitial infiltration of inflammatory cells. Epithelial cell injury appeared to occur around Day 9 after BLM treatment. In addition, intratracheal administration of BLM (5 mg/kg) significantly decreased the survival rate, and seven mice died before Day 17. We evaluated the effect of NKM in this model and compared it with that of Dex. Dex (1 mg/kg) did not improve the survival rate, consistent with the previous report [27]. In contrast, NKM (2 mg/kg) improved the survival rate significantly over the 17-day period. Some reports have shown that treatment with Dex does not inhibit lung injury induced by several kinds of toxins, including BLM [28,29]. One possible explanation is that Dex is not beneficial at an early stage of acute lung injury [30]. In our model, however, Dex was not tolerated in mice treated with BLM, and Dex and NKM both suppressed the total number of cells, neutrophils, and lymphocytes in the blood when compared with saline, in agreement with the previous study [31]. Furthermore, NKM inhibited a significantly greater number of neutrophils than Dex, suggesting that the difference in survival rate observed between Dex therapy and NKM therapy may depend partly on their different abilities to inhibit neutrophils. *In vitro*, transfer and expression of the NIF gene in endothelial and epithelial cells can prevent the adhesion of neutrophils [32]. *In vivo*, when mice were challenged with *E. coli*, inflammation-specific NIF expression induced by the E-selectin promoter prevented lung PMN sequestration and vascular injury [33]. In the $NIF^{+/+}$-mouse transgenic model, CD11b inactivation as a result of binding to NIF interfered with lung PMN infiltration and prevented increases in lung microvessel permeability and edema formation [34]. In acid-induced lung injury in rabbits mediated primarily by activated neutrophils, pretreatment (5 min before acid treatment) with NIF prevented 50–70% of the acid-induced abnormalities in oxygenation and an increase in extravascular water and protein accumulation in the lung [35]. These studies suggest that neutrophil-dominated inflammation in the lungs contributes to the pathophysiology of pulmonary fibrosis. This indicates that adhesion plays a crucial role in mediating lung PMN sequestration and vascular injury in the early phase of lung injury [34]. NKM treatment is beneficial to BLM-evoked acute lung injury because of NKM's capacity to reduce neutrophil activation and cell counts.

KGF is a potent mitogen that enhances cell proliferation in various organs, including the skin, intestines, breasts, liver, and lungs [36]. Intratracheal instillation of KGF causes transient, but marked, epithelial cell hyperplasia of

both bronchiolar and alveolar epithelial cells in the lungs of rats and mice. Following KGF treatment, cell proliferation peaks in 2–3 days [37]. As KGF has marked promitotic activity in respiratory epithelial cells, its potential utility for the prevention or treatment of lung injury has been explored *in vivo* [38]. Pretreatment of the lung with KGF protects animals from the various effects of oxygen-, acid-, BLM-, or radiation-induced lung injury [39]. Additionally, an increase in KGF levels has been observed in injured lungs [40], suggesting that KGF has important functions in regulating the response of the lung to injury. The exact mechanisms of the protective effect of KGF have not yet been elucidated, but various mechanisms appear to be involved. KGF induces the proliferation of alveolar epithelial type II cells, stabilizes surfactant homeostasis, improves the barrier function of both vascular endothelia and alveolar epithelia, increases fluid clearance from the alveoli, limits lung permeability, and causes an anti-inflammatory effect [41]. Therefore, we speculate that NKM exerts its protective action by inhibiting the proliferation of fibroblasts together with other anti-inflammatory properties. Of course, various other mechanisms may also contribute to the ameliorative effects on lung injury, as the decreases in mouse mortality and the improvements in lung hydroxyproline levels and morphological indices for assessing lung fibrosis in BLM-induced mice have confirmed (**Figs. 8 and 9**). The NKM fusion protein, which was constructed by connecting a KGF mutant via an octapeptide to the C-terminal of NIF, was found to be a good design, and our method is scalable to the preparation of large quantities of biologically active recombinant NKM fusion protein, which will enable its future application in preclinical and clinical studies on pulmonary fibrosis.

Acknowledgements

We gratefully acknowledge Prof. Fan Kai who kindly presented us with NIF, KGF, and the primary antibodies. We thank Hongqi Huo, Hailian Qiao, and Prof. Zhifa Yuan for their help with the experiments and statistical analysis.

Funding

This work was supported by a grant from National Nature Science Foundation of China (30471250).

References

1 Miki T, Bottaro DP, Fleming TP, Smith CL, Burgess WH, Chan AM and Aaronson SA. Determination of ligand-binding specificity by alternative splicing: two distinct growth factor receptors encoded by a single gene. Proc Natl Acad Sci USA 1992, 89: 246–250.

2 Finch PW, Cunha GR, Rubin JS, Wong J and Ron D. Pattern of keratinocyte growth factor and keratinocyte growth factor receptor expression during mouse fetal development suggests a role in mediating morphogenetic mesenchymal-epithelial interactions. Dev Dyn 1995, 203: 223–240.

3 Yi ES, Williams ST, Lee H, Malicki DM, Chin EM, Yin S and Tarpley J. Keratinocyte growth factor ameliorates radiation and bleomycin-induced lung injury and mortality. Am J Pathol 1996, 149: 1963–1970.

4 Simonet WS, Derose ML, Bucay N, Nguyen HQ, Werti SE, Zhou L and Ulich TR, *et al*. Pulmonary malformation in transgenic mice expressing human keratinocyte growth factor in the lung. Proc Natl Acad Sci USA 1995, 92: 12461–12465.

5 Gomperts BN, Belperio JA, Fishbein MC, Keane MP, Burdick MD and Strieter RM. Keratinocyte growth factor improves repair in the injured tracheal epithelium. Am J Respir Cell Mol Biol 2007, 37: 48–56.

6 Barnard JW, Biro MG, Lo SK, Ohno S, Carozza MA, Moyle M and Soule HR, *et al*. Neutrophil inhibitory factor prevents neutrophil-dependent lung injury. J Immunol 1995, 155: 4876–4881.

7 Madden K, Janczak J, McEnroe G, Lim D, Hartman T, Liu D and Stanton L. A peptide derived from neutrophil inhibitory factor (NIF) blocks neutrophil adherence to endothelial cells. Inflamm Res 1997, 46: 216–223.

8 Zhou MY, Lo SK, Bergenfeldt M, Tiruppathi C, Jaffe A, Xu N and Malik AB. *In vivo* expression of neutrophil inhibitory factor via gene transfer prevents lipopolysaccharide-induced lung neutrophil infiltration and injury by a beta2 integrin-dependent mechanism. J Clin Invest 1998, 101: 2427–2437.

9 Antoniou KM, Pataka A, Bouros D and Siafakas NM. Pathogenetic pathways and novel pharmacotherapeutic targets in idiopathic pulmonary fibrosis. Pulm Pharmacol Ther 2007, 20: 453–461.

10 Cabrera S, Gaxiola M, Arreola JL, Ramírez R, Jara P, Armiento JD and Richards T, *et al*. Overexpression of MMP9 in macrophages attenuates pulmonary fibrosis induced by bleomycin. Int J Biochem Cell Biol 2007, 39: 2324–2338.

11 Knight DA, Ernst M, Anderson GP, Moodley YP and Mutsaers SE. The role of gp130/IL-6 cytokines in the development of pulmonary fibrosis: critical determinants of disease susceptibility and progression? Pharmacol Ther 2003, 99: 327–338.

12 Laemmli UK. Cleavage of structural protein during the assembly of the head of bacteriophage T4. Nature 1970, 227: 680–685.

13 Ma HH, Li Y, Yang XY, Xu ZP and Li BL. Bacterial expression, purification, and in vitro N-myristoylation of fusion hepatitis B virus preS1 with the native-type N-terminus. Protein Expr Purif 2003, 27: 49–54.

14 Ringertz B, Palmblad J and Lindgren JÅ. Stimulus specific neutrophil aggregation − evaluation of possible mechanism for the stimulus-response apparatus. J Lab Clin Med 1985, 106: 132–140.

15 Bullido R, Alonso F, Moral MG, Ezquerra A, Alvarez B, Ortufo E and Dominguez J. Monoclonal antibody 2F4/11 recognizes the alpha chain of a porcine beta 2 integrin involved in adhesion and complement mediated phagocytosis. J Immunol Methods 1996, 195: 125–134.

16 Soguta S, Ozyurtb H, Armutcuc F, Kartd L, Iraze M, Akyolf O and Ozeng S, *et al*. Erdosteine prevents bleomycin-induced pulmonary fibrosis in rats. Eur J Pharmacol 2004, 494: 213–220.

17 auf dem Keller D. Keratinocyte growth factor: effects on keratinocytes and mechanisms of action. Eur J Cell Biol 2004, 83: 607–612.

18 Dorra W, Reichela S and Spekl K. Effects of keratinocyte growth factor (palifermin) administration protocols on oral mucositis (mouse) induced by fractionated irradiation. Radiother Oncol 2005, 75: 99–105.

19 Hsu E, Osslund T, Nybo R, Chen BL, Kenney WC, Morris CF and Arakawa T, *et al*. Enhanced stability of recombinant keratinocyte growth factor by mutagenesis. Protein Eng Des Sel 2006, 19: 147–153.

20 Fehrenbach H, Fehrenbach A, Dietzel E, Tschernig T, Krug N, Grau V and Hohlfeld JM. Effects of keratinocyte growth factor on intra-alveolar

surfactant fixed in situ: quantitative ultrastructural and immunoelectron microscopic analysis. Anat Rec 2007, 290: 974–980.
21 Tang A and Gilchrest BA. Regulation of keratinocyte growth factor gene expression in human skin fibroblasts. J Dermatol Sci 1996, 11: 41–50.
22 Kuan YH, Lin RH, Chen YL, Tsao LT, Tzeng CC and Wang JP. Effective attenuation of acute lung injury in vivo and the formyl peptide-induced neutrophil activation in vitro by CYL-26z through the phosphoinositide 3-kinase γ pathway. Biochem Pharmacol 2006, 72: 749–760.
23 Lo SK, Rahman A, Xu N, Zhou MY, Nagpala P, Jaffe HA and Malik AB. Neutrophil inhibitory factor abrogates neutrophil adhesion by blockade of CD11a and CD11b β_2 integrins. Mol Pharmacol 1999, 56: 926–932.
24 Gong ZH, Long X, Lin P, Le YP, Liu Q, Wang SM and Guo JM, *et al*. Cloning, expression, purification and characterization of the cholera toxin B subunit and triple glutamic acid decarboxylase epitopes fusion protein in *Escherichia coli*. Protein Expr Purif 2009, 66: 191–197.
25 Moeller A, Askc K, Warburton D, Gauldie J and Kolb M. The bleomycin animal model: a useful tool to investigate treatment options for idiopathic pulmonary fibrosis. Int J Biochem Cell Biol 2008, 40: 362–382.
26 Chaudhary NI, Schnapp A and Park JE. Pharmacologic differentiation of inflammation and fibrosis in the rat bleomycin model. Am J Respir Crit Care Med 2006, 173: 769–776.
27 Koshikaa T, Hirayamaa Y, Ohkuboa Y, Mutoha S and Ishizakab A. Tacrolimus (FK506) has protective actions against murine bleomycin-induced acute lung injuries. Eur J Pharmacol 2005, 515: 169–178.
28 Wang XH, Ding XC and Wang Z. Experimental study on effect of stronger NEO-minophagen C in treating rats with bleomycin-induced pulmonary fibrosis. Chin Arch Trad Chin Med 2008, 26: 2628–2670.
29 Wang SJ, Bai W, Wang CL and Dai Z. Experimental study on effect of Huaxian decoction in treating bleomycin-induced pulmonary fibrosis in mice. Chin J Integr Trad West Med 2007, 27: 347–351.
30 Bernard GR, Luce JM, Sprung CL, Rinaldo JE, Tate RM, Sibbald WJ and Kariman K, *et al*. High-dose corticosteroids in patients with the adult respiratory distress syndrome. N Engl J Med 1987, 317: 1565–1570.
31 Jeklova E, Leva L, Jaglic Z and Faldyna M. Dexamethasone-induced immunosuppression: a rabbit model. Vet Immunol Immunopathol 2008, 122: 231–240.
32 Jaffe HA, Nagpala PG, Yu JC, Gao ZC and Malik AB. Transfer and expression of neutrophil inhibitory factor gene in endothelial and epithelial cells prevent neutrophil adhesion. Chest 1997, 111: 94–95.
33 Xu N, Rahman A, Minshall RD, Tiruppathi C and Malik AB. β_2-Integrin blockade driven by E-selectin promoter prevents neutrophil sequestration and lung injury in mice. Circ Res 2000, 87: 254–260.
34 Gao XP, Liu QH, Broman M, Predescu D, Frey RS and Malik AB. Inactivation of CD11b in a mouse transgenic model protects against sepsis-induced lung PMN infiltration and vascular injury. Physiol Genomics 2005, 21: 230–242.
35 Folkesson HG and Matthay MA. Inhibition of CD18 or CD11b attenuates acute lung injury after acid instillation in rabbits. J Appl Physiol 1997, 82: 1743–1750.
36 Luo YD, Cho HH, Jones RB, Cheng LJ and McKeehana WL. Improved production of recombinant fibroblast growth factor 7 (FGF7/KGF) from bacteria in high magnesium chloride. Protein Expr Purif 2004, 33: 326–331.
37 Ulich TR, Yi ES, Longmuir K, Yin S, Biltz R, Morris CF and Housley RM, *et al*. Keratinocyte growth factor is a growth factor for type II pneumocytes *in vivo*. J Clin Invest 1994, 93: 1298–1306.
38 Baba Y, Yazawa T, Kanegae Y, Sakamoto S, Saito I, Morimura N and Goto T, *et al*. Keratinocyte growth factor gene transduction ameliorates acute lung injury and mortality in mice. Hum Gene Ther 2007, 18: 130–141.
39 Tichelaar JW, Lu W and Whitsett JA. Conditional expression of fibroblast growth factor-7 in the developing and mature lung. J Biol Chem 2000, 275: 11858–11864.
40 Adamson IYR and Bakowska J. Relationship of keratinocyte growth factor and hepatocyte growth factor levels in rat lung lavage fluid to epithelial cell regeneration after bleomycin. Am J Pathol 1999, 155: 949–954.
41 Grau V, Wilker S, Hartmann P, Lips KS, Grando SA, Padberg W and Fehrenbach H, *et al*. Administration of keratinocyte growth factor (KGF) modulates the pulmonary expression of nicotinic acetylcholine receptor subunits α7, α9 and α10. Life Sci 2007, 80: 2290–2293.